

# TRANSITION CROSSING

Elias Métral and Dieter Möhl

## INTRODUCTION

The CERN PS is one of the first synchrotrons where transition had to be crossed. This occurred for the first time during the night of November 24<sup>th</sup>, 1959, when a beam with an intensity of  $\sim 10^{10}$  protons was accelerated through transition up to the top energy of 25 GeV. However, between the day when transition crossing was first tried, and this famous night, quite some time elapsed, during which the machine specialists oscillated between few triumphant moments and most of the time discouragement. It seemed as if the protons just did not want to be accelerated through transition. Eventually, the breakthrough, and the relief of all the PS early workers, came from Schnell's Nescafé tin. The idea was to use the radial-position signal from the beam to control the RF phase instead of the amplitude. Such a system for the PS had been contemplated before [1], but the early running-in was done without it. Then, in great haste, W. Schnell built the missing parts for phase control into a Nescafé tin and, when this device was branched, the beam could readily be accelerated through transition up to top energy [2]. A similar phase-system would then be used in the AGS a few months later, and in all the subsequent synchrotrons where transition had to be crossed.

But, what is the origin of transition and what are the difficulties to cross it? The increase of energy in a synchrotron such as the CERN PS has two contradictory effects: (i) an increase of the particle's velocity and (ii) an increase of the length of the particle's trajectory. According to the variations of these two parameters, the revolution frequency evolves differently. Below a certain energy, called transition energy, the velocity increases faster than the length: the revolution frequency increases. Above transition energy, the opposite is true (at very high energy the velocity reaches the speed of light and does not change anymore): the revolution frequency decreases. At transition energy, the variation of the velocity is compensated by the variation of the trajectory: a variation of energy does not modify the revolution frequency. This is the isochronous condition.

The ratio between the beam energy at transition and the rest energy of the particles, called  $\gamma_t$  (relativistic mass factor at transition), is independent of the particle mass. Its value depends only on the machine optics and geometry and is given by

$$\gamma_t = \frac{1}{\sqrt{\alpha_p}} \quad \text{with} \quad \alpha_p = \frac{dC / C_0}{dp / p_0}, \quad (1)$$

where  $C_0$  is the circumference of a particle with nominal momentum  $p_0$  on the reference orbit (the parameter  $\alpha_p$  is called the momentum compaction factor). In the case of a regular lattice, the value of  $\gamma_t$  is close to the horizontal tune,  $\gamma_t \approx Q_x$ . This is the case in the PS where the horizontal tune is  $Q_x \approx 6.25$  and  $\gamma_t \approx 6.1$ . In fact, due to the transverse space-charge force, which modifies the tune of each individual particle,  $\gamma_t$  depends on the azimuthal beam density. Therefore, all the particles do not cross transition simultaneously. However, this so-called Umstätter effect [3, p. 285] is usually negligible if the transition energy is much bigger than the injection energy. The chromatic nonlinearities also produce a spread in the  $\gamma_t$  value of the particles, which is known as the Johnsen effect [3, p. 285] and can be reduced using sextupole families.

Crossing transition changes the sign of the slip factor (which relates the frequency spread in the beam to its momentum spread) given by

$$\eta = \alpha_p - \frac{1}{\gamma^2} = -\frac{\Delta f / f_0}{\Delta p / p_0}, \quad (2)$$

where  $f_0 = \Omega_0 / 2\pi$  is the revolution frequency of a particle with nominal momentum on the reference orbit. As the small-amplitude (in one RF bucket) synchrotron angular frequency is given by

$$\omega_s = \Omega_0 \left( -\frac{e \hat{V}_{RF} h \eta \cos \phi_s}{2\pi \beta^2 E_{total}} \right)^{1/2}, \quad (3)$$

where  $e$  is the elementary charge,  $\hat{V}_{RF}$  the peak RF voltage,  $h$  the RF harmonic number,  $\phi_s$  the synchronous phase,  $\beta$  the relativistic velocity factor and  $E_{total} = \gamma E_{rest}$  the total energy of the synchronous particle having the rest energy  $E_{rest}$ , the sign of  $\cos \phi_s$  has to be changed to keep  $-\eta \cos \phi_s \geq 0$  and maintain the longitudinal phase stability. This means that as a first consequence of transition crossing, the synchronous phase has to jump rapidly from  $\phi_s$  to  $\pi - \phi_s$ .

## NUMEROUS UNFAVOURABLE EFFECTS

### *Nonadiabatic region*

Because of its dependence on  $\eta$ , the synchrotron frequency slows down near the transition region, and the

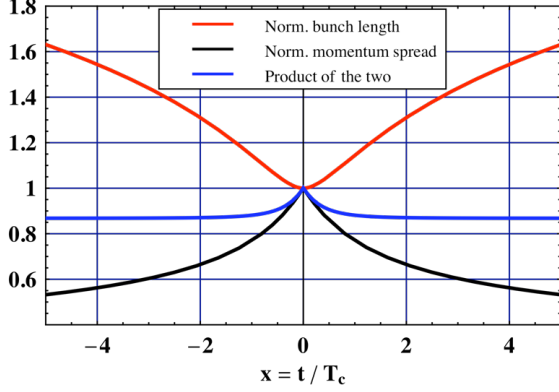


Figure 1: Evolution of the bunch length and momentum spread normalized to their values at transition plotted as functions of time measured from transition in units of the nonadiabatic time.

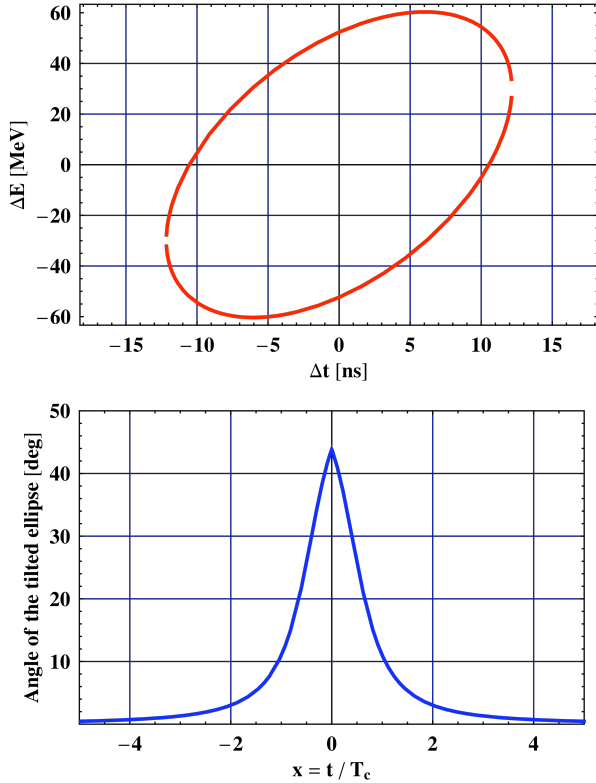


Figure 2: (Upper) tilted longitudinal phase space ellipse right at transition and (lower) evolution of the tilted angle around transition, both for the case of the PS nTOF bunch (see Table 1).

adiabaticity condition

$$\frac{1}{\omega_s^2} \left| \frac{d\omega_s}{dt} \right| \ll 1, \quad (4)$$

where  $t$  is time, is not satisfied anymore, which results in a nonadiabatic synchrotron motion. The nonadiabatic time is defined as [4]

$$T_c = \left( \frac{\beta^2 E_{rest} \gamma_t^4}{4 \pi f_0^2 \dot{\gamma} h \hat{V}_{RF} |\cos \phi_s|} \right)^{1/3}, \quad (5)$$

where  $\dot{\gamma} = d\gamma / dt$ . The physical meaning of it is that when the time is close enough to transition, the particle will not be able to catch up with the rapid modification of the bucket shape. It can be shown analytically that the bunch length reaches a minimum right at transition (see Fig. 1), which is not zero as could be deduced from the adiabatic theory (see Fig. 3), while the momentum spread reaches a maximum and can become so large that it exceeds the available momentum aperture, causing beam losses [4-6]. As the product of the bunch length and momentum spread in Fig. 1 is not constant it can be already anticipated that the longitudinal phase space ellipse is tilted near transition, as it is confirmed in Fig. 2 for the case of the PS nTOF bunch (see Table 1) [7], for which the nonadiabatic time is  $T_c \approx 1.9$  ms. It's worth emphasising that all the curves in Fig. 1 are symmetric with respect to the transition time.

Average machine radius: $R$ [m]	100
Bending dipole radius: $\rho$ [m]	70
$\dot{B}$ [T/s]	2.2
$\hat{V}_{RF}$ [kV]	200
$h$	8
$\alpha_p$	0.027
Longitudinal (total) emittance: $\epsilon_L$ [eVs]	2
Number of protons/bunch: $N_b$ [1E10 p/b]	800
Norm. rms. transverse emittance: $\epsilon_{x,y}^*$ [ $\mu\text{m}$ ]	5
Trans. average betatron function: $\beta_{x,y}$ [m]	16
Beam pipe [cm $\times$ cm]	3.5 $\times$ 7
Trans. tunes: $Q_{x,y}$	6.25

Table 1: Relevant parameters for the PS and nTOF bunch.

### *Nonlinear synchrotron motion*

A second effect arises from the nonlinearities in the slip factor. Equation (1) only gives the linear dependence of the orbit length on momentum offset. In the general case, it should be extended to [4]

$$C(\delta) = C_0 \left[ 1 + \alpha_0 \delta \left( 1 + \alpha_1 \delta + \alpha_2 \delta^2 + \dots \right) \right], \quad (6)$$

where  $\delta = \Delta p / p_0$  and  $\alpha_1$ ,  $\alpha_2$ , etc. are called the high-order components of the momentum compaction factor. Thus, the slip factor  $\eta$  becomes now also momentum spread dependent and this raises another nonlinear problem in synchrotron motion. To characterize this nonlinear synchrotron motion, a nonlinear time  $T_{nl}$  can be defined as the time when the phase slip factor changes sign for the particle at the maximum momentum width of the beam [5]. Within  $\pm T_{nl}$ , some portions of the beam could experience unstable synchrotron motion.

### Longitudinal mismatch

A third adverse effect comes from the longitudinal Space Charge (SC) and/or the inductive part of the

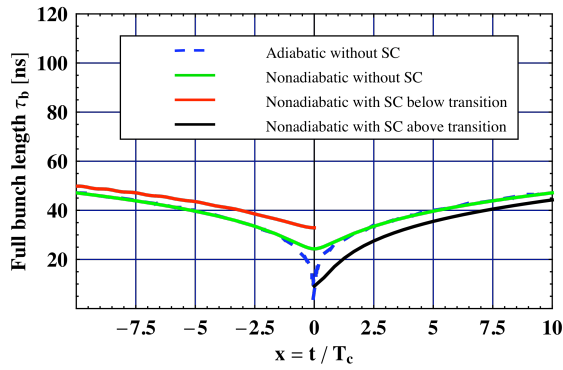


Figure 3: Evolution of the full bunch length vs. time for the case of the adiabatic theory without Space Charge (SC), and for the nonadiabatic theory with and without SC in the static case (i.e. without crossing transition), applied to the PS nTOF bunch.

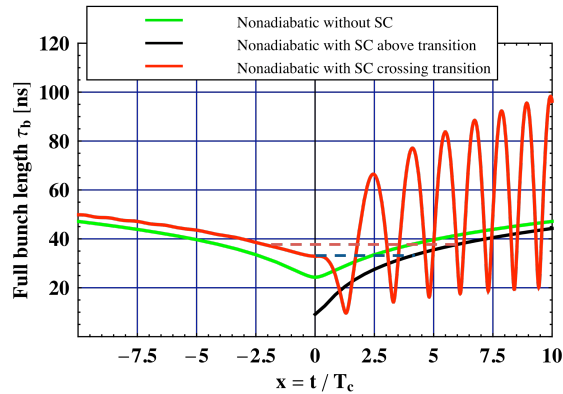


Figure 4: Evolution of the full bunch length vs. time for the case of the nonadiabatic theory with and without Space Charge (SC) in the dynamic case (i.e. crossing transition), applied to the PS nTOF bunch.

longitudinal Broad-Band (BB) impedance. Considering first only SC, as it is defocusing below transition and focusing above, the equilibrium bunch length below transition is longer than without SC, while it is shorter above (see Fig. 3, which has been obtained by solving numerically the longitudinal envelope equation near transition). Therefore, there is an intensity-dependent step in the equilibrium bunch length at transition, which leads to a longitudinal mismatch and subsequent quadrupolar oscillations when transition is crossed (see Fig. 4) [8]. If these bunch shape oscillations are not damped they will eventually result in filamentation and longitudinal emittance blow-up. It's worth mentioning that in the case of Fig. 4, the minimum of bunch length is not reached right at transition anymore, but after about one nonadiabatic time, i.e. after  $\sim 2$  ms in the present case. The same kind of mechanism appears with the inductive part of the longitudinal BB impedance (see Fig. 5). The difference with the case of SC, is that the equilibrium bunch length is now shorter (than without impedance) below transition and longer above transition, i.e. it is the opposite of SC. Therefore, the inductive part of the longitudinal impedance can be used to compensate the SC effect. Furthermore, the minimum bunch length in this case is reached right at transition. Measuring the evolution of the bunch length near transition in a machine (with both SC and BB impedance) can provide some information about the inductive part of the machine BB impedance. However, as the BB impedance of a machine also has some real part, the previous analysis is valid only below a certain intensity threshold, as above it a longitudinal coherent instability will develop.

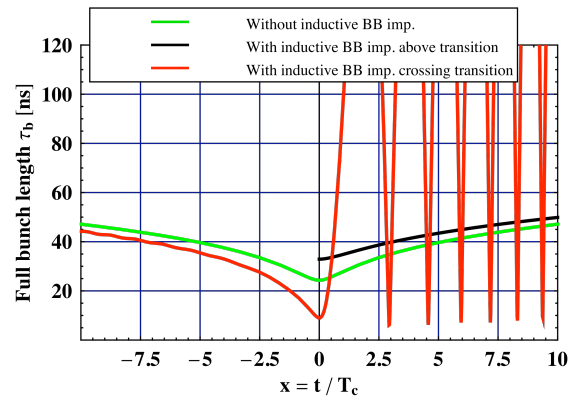


Figure 5: Evolution of the full bunch length vs. time for the case of the nonadiabatic theory with (only) and without an inductive Broad-Band impedance (BB) in the dynamic case (i.e. crossing transition), applied to the PS nTOF bunch. Here a BB impedance of  $Z_l^{BB} / n = j 20 \Omega$  has been used.

## Head-Tail instability

A fourth impediment to transition crossing with high-intensity beams comes from the transverse head-tail instability. If the sign of the chromaticity (which is equal to  $\sim -1$  for an uncorrected machine like the PS) is not changed (in both transverse planes) above transition, a (single-bunch) head-tail instability may develop [9-11]. This instability can be damped through Landau damping using octupoles, which introduce some amplitude detunings. This method was first used in the past to stabilize the PS beams. However, the better method of changing the sign of the chromaticities (and keeping them to small positive values, usually between  $\sim 0.05$  and  $\sim 0.1$ ) by acting on the optics with sextupoles was then adopted, and it has become a routine operation at the CERN PS for many years.

### Negative mass and microwave instabilities

Finally, since the frequency spread of the beam vanishes at transition energy (see Eq. (2)), there is no (or little, depending on nonlinearities) Landau damping of the longitudinal and transverse microwave instabilities which can lead to emittance growth and / or huge beam losses [3, p.119]. It was Lee and Teng who pointed first to the importance of the microwave (negative mass) instability [12].

## REMEDIES

To avoid all the above unfavourable effects, it is appealing to eliminate transition crossing. Nowadays, an accelerator lattice can be designed in such a way that the momentum compaction factor  $\alpha_p$  is negative (as for instance the CERN LEAR machine), and thus the beam never encounters transition energy. This is called the “Negative Momentum Compaction” (NMC) or the “imaginary  $\gamma_t$ ” lattice. The NMC modules were invented by Teng [13] and were later pushed by Trbojevic et al. [14].

On the other hand, the  $\gamma_t$  value of existing machines such as the PS cannot be changed by a large amount without changing the ring geometry. Many compensation methods have been studied in the past [3, p. 285], such as for instance the “triple switch” scheme [15], where the RF phase is switched back and forth three times to try and cure the bunch tumbling from the longitudinal SC (see Fig. 4). The idea is that after switching the phase from  $\phi_s$  to  $\pi - \phi_s$  at the transition time  $x_1 = 0$ , the bunch tries to adjust itself to fit the configuration of shorter bunch length. At some time  $x_2$  before the undershoot, the phase is switched back to  $\phi_s$ . The bunch is then at an unstable fixed point and it will try to lengthen. The phase

is finally switched back to  $\pi - \phi_s$  at the time  $x_3$ , chosen such that the bunch lengthening cancels the undershoot thus damping out the oscillations and eventual filamentation. However, this method has not been successfully implemented in the CERN PS because it does not work at high intensity, by principle, due to the spread in  $\gamma_t$ : the required precision on the different timings  $x_{1,2,3}$  can be achieved for a group of particles but not for all of them. Moreover, the negative mass instability (and probably also the head-tail instability) was still a pending issue. Note that a feedback device can also be used to damp out the longitudinal quadrupolar oscillations, but as was seen previously, many other effects are detrimental.

### $\gamma_t$ jump

If transition crossing cannot be avoided, the  $\gamma_t$  jump is the only (known) method to overcome all the intensity limitations resulting from the above-mentioned phenomena. It consists in an artificial increase of the transition crossing speed by means of fast pulsed quadrupoles. The idea is that quadrupoles at nonzero dispersion locations can be used to adjust the momentum compaction factor  $\alpha_p$ . The change in momentum compaction (called  $\gamma_t$  jump) depends on the unperturbed and perturbed dispersion functions at the kick-quadrupole locations. These schemes were pioneered by the CERN PS group [16-18]. Such a  $\gamma_t$  jump scheme makes it possible to keep the beam at a safe distance from transition, except for the very short time during which the transition region is crossed at a speed increased by one or two orders of magnitude (see Fig. 6). The required jump amplitude and speed depend on the beam intensity. In the present case of the PS, the transition crossing speed without  $\gamma_t$  jump is  $\dot{\gamma} = 49.9 \text{ s}^{-1}$ , whereas the effective crossing speed  $\dot{\gamma}_{eff} = \dot{\gamma} - \dot{\gamma}_t$  in the presence of the  $\gamma_t$  jump becomes  $\sim 50 \dot{\gamma}$ , i.e. about 50 times faster than

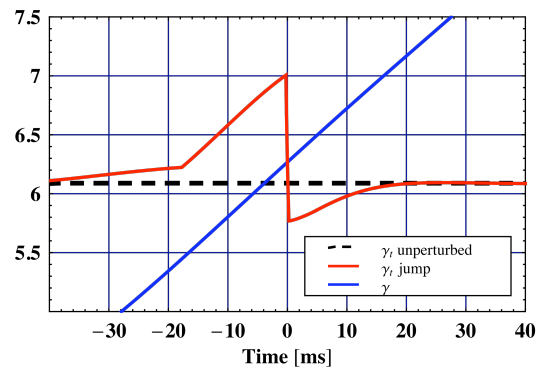


Figure 6: Evolution of  $\gamma_t$  (and of the  $\gamma$  of the beam) near transition crossing without and with the present PS  $\gamma_t$  jump.

without jump. The amplitude of the  $\gamma_t$  jump is  $\Delta\gamma_t \approx -1.24$  and the jump time is  $\Delta t_{\text{jump}} \approx 500 \mu\text{s}$  (see also Fig. 7).

Looking at Fig. 4 clearly reveals why an asymmetric jump was proposed in the past [17] to damp the longitudinal quadrupolar oscillations arising from the SC induced mismatch: the idea is to jump rapidly from an equilibrium bunch length below transition to the same value above. The amplitude of the jump is defined by the time between the same equilibrium bunch length below and above transition. The minimum amplitude of the jump corresponds to the case represented with the dashed blue line starting right at transition. However, in this case the initial longitudinal phase space ellipse is tilted (see Fig. 2), while the final one is almost not, which is not ideal. One might want therefore to start the jump earlier, when the longitudinal phase space is almost not tilted, for instance at  $x = -2$ , which requires a larger jump (see the dashed orange line in Fig. 4). Finally, taking into account the longitudinal and transverse microwave instabilities, whose intensity thresholds are proportional to  $|\eta|$  [19], even larger jumps might be required. The evolution of  $\eta$  near transition crossing with the present PS  $\gamma_t$  jump is depicted in Fig. 7. As can be seen, a minimum value of  $|\eta_{\text{min}}| \approx 5 \times 10^{-3}$  is always obtained except for the very

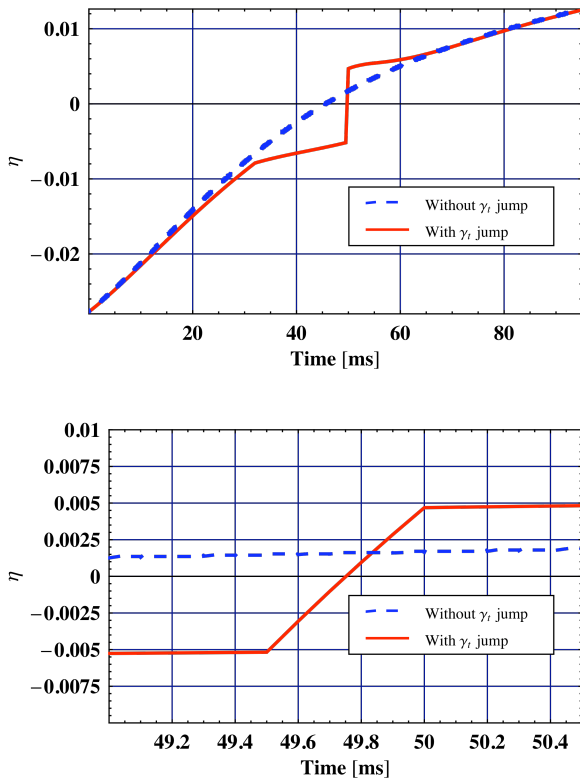


Figure 7: (Upper) evolution of  $\eta$  near transition crossing with the present PS  $\gamma_t$  jump, and (lower) zoom.

short time of the jump, i.e. during  $\Delta t_{\text{jump}} \approx 500 \mu\text{s}$ . In the absence of the  $\gamma_t$  jump,  $|\eta|$  would have been smaller than  $|\eta_{\text{min}}|$  during  $\sim 25$  ms.

### Review of the PS $\gamma_t$ jump schemes [20]

Up to 1960, transition in the PS was crossed without a  $\gamma_t$  jump practically as on the first night in 1959. When the intensity had approached  $10^{12}$  protons per pulse, a blow-up of the longitudinal emittance occurred due to several of the effects discussed above. Various antidotes, including the triple phase switch, brought no radical improvement, until in 1969 the so-called Q-jump scheme [16,17] was introduced. A nonzero tune shift was tolerated and  $\gamma_t \approx Q_x$  was ‘jumped’ using a set of 6 quadrupoles more or less regularly spaced around the ring with identical strengths and polarities. A tune change of  $\Delta Q_x = 0.25$  was required to obtain a  $|\Delta\gamma_t| = 0.3$ . The fast part of the jump (Fig. 8) took place in about 2 ms.

In 1970, a scheme was proposed for the FNAL Booster using 12 regularly spaced quadrupoles with equal strengths but alternating polarities [21], yielding  $|\Delta\gamma_t| = 1$  at the expense of only  $\Delta Q_x = 0.1$ . It was again Teng who emphasised that one can/should change  $\gamma_t$  without changing  $Q_x$ , which led to the birth of the  $\gamma_t$  jump. The idea was enthusiastically taken up by Hardt and collaborators and the scheme for the PS conceived.

Since 1973, a large  $\gamma_t$  jump ( $|\Delta\gamma_t| \approx 1.2$ ) with (almost) zero tune shift is obtained in the PS by grouping 16 quadrupoles (with two strengths  $\pm K_1$  and  $\pm K_2$ ) together in doublets. The use of quadrupole pairs separated by  $\pi$  in the betatron phase advance (called  $\pi$ -doublets) gives zero tune shift and avoid nonlinear betatron resonances crossing. The fast part of the jump takes place in about 0.5 ms. Note that during the  $\gamma_t$  jump the dispersion function has the tendency to increase. This can lead to an increase of the horizontal beam size and a subsequent beam loss. The optical design of a  $\gamma_t$  jump scheme should therefore aim at a large  $\Delta\gamma_t$ , while keeping the maximum dispersion and betatron functions

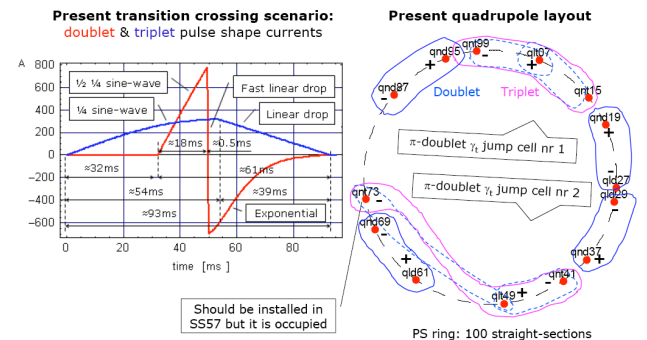


Figure 8: Present transition crossing scheme in the PS.

below reasonable values, and the tune shift should be as small as possible. Transition crossing with a  $\gamma_t$  jump has become a routine operation at the CERN PS, where the present scheme is shown in Fig. 8 [22,23].

In normal operation, total intensities up to few  $10^{13}$  protons (in several bunches) can be passed without too much blow-up through transition. However, for the nTOF operation with an extremely dense bunch (see Table 1), even in the presence of this  $\gamma_t$  jump, together with the change of the sign of both chromaticities when transition is crossed, a fast vertical single-bunch instability is observed when no longitudinal emittance blow-up is applied before transition (see Fig. 9) [19,24]. Figure 9 reveals that the head of the bunch (on the left) is stable and only the tail is unstable in the vertical plane. The particles lost at the tail of the bunch can be seen from the hollow in the bunch profile. The remedy that was found and applied since then is to increase (before transition crossing) the longitudinal emittance from  $\sim 1.5$  eVs to  $\sim 2.1$  eVs for an intensity of  $\sim 7 \times 10^{12}$  p/b [24]. However, this can only be done because the longitudinal emittance is not a critical parameter for this beam. If one would have no margin in the longitudinal emittance the  $\gamma_t$  jump should be improved with a larger amplitude and an increased speed. A possible alternative could be to not only change the sign of the chromaticities as proposed in Refs. [9-11] for (slow) head-tail considerations but to correlate the variation of the chromaticity with the one of the slip factor, for (fast) head-tail considerations this time [25].

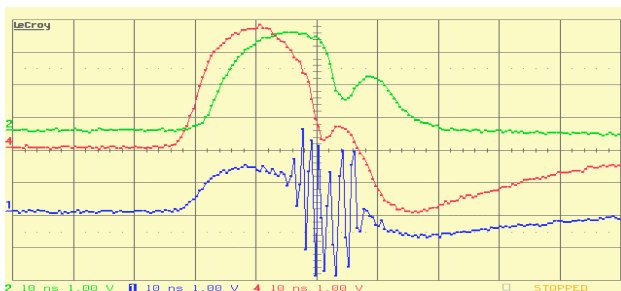


Figure 9: Single-turn signals from a wide-band pick-up in the CERN PS in 2000 with the nTOF bunch. From top to bottom:  $\Sigma$ ,  $\Delta x$ , and  $\Delta y$ . Time scale: 10 ns/div.

## LESSONS LEARNED FROM THE PS

Since the bunch length becomes naturally very short near transition, operating synchrotrons under an isochronous or quasi-isochronous condition has been proposed to achieve very short bunches in numerous future projects. These designs require both an accurate control of the first high-order component of the momentum compaction factor  $\alpha_1$  (using sextupoles) to

provide the necessary momentum acceptance and effective ways to damp all the collective instabilities.

## REFERENCES

- [1] See e.g. K. Johnsen and C. Schmelzer, "Beam Controlled Acceleration in Synchrotrons", CERN Symposium on H.E. Accelerators and Pion-Physics, June 1956 (395); E. Regenstreif, "Le Synchrotron à protons du CERN (1ère partie)", 1 juillet 1958, CERN Report 58-06A; W.Schnell, "Remarks on the Phase-Lock System of the CPS", Int.Conf.on HE Accelerators and Instrumentation, CERN, 14-19 September 1959 (485).
- [2] CERN Proton Synchrotron Machine Group, "Operation and Development, Quarterly Report No.1", p. 6 ff., CERN Report 60-23. See also CERN Courier, No. 11, Vol. 19, November 1969 (10<sup>th</sup> anniversary of the first operation of the CERN Proton Synchrotron).
- [3] J. Wei, "Transition Crossing", in "Handbook of Accelerator Physics and Engineering" (edited by A.W. Chao and M. Tigner), World Scientific, 2<sup>nd</sup> Printing (2002).
- [4] K.Y. Ng, "Physics of Intensity Dependent Beam Instabilities", World Scientific (2006), p. 691.
- [5] S.Y. Lee, "Accelerator Physics", World Scientific (1999), p. 275.
- [6] E. Métral, USPAS course on "Collective Effects in Beam Dynamics" in Albuquerque, New Mexico, USA, June 22-26, 2009: <http://uspas.fnal.gov/materials/09UNM/CollectiveEffects.html>.
- [7] S. Andriamonje *et al.*, "Neutron TOF Facility (PS213): Technical Design Report", CERN-INTC-2000-004, 2000.
- [8] A. Sorensen, "Longitudinal Space-Charge Forces at Transition", Proc. 6<sup>th</sup> Int. Conf. on High Energy Accelerators (1967), p. 474.
- [9] M. Sands, "The Head-Tail Effect: An Instability Mechanism in Storage Rings", SLAC-TN-69-8, 1969.
- [10] M. Sands, "Head-Tail Effect II: From a Resistive-Wall Wake", SLAC-TN-69-10, 1969.
- [11] C. Pellegrini, Nuovo Cimento 64A, 477, 1969.
- [12] W.W. Lee and L.C. Teng, Proc. 8<sup>th</sup> Int. Conf. on High En. Acc., CERN, p. 327, 1971.
- [13] L.C. Teng, "Infinite Transition-Energy Synchrotron Lattice using PI-Straight Sections", Part. Accel. **4**, p. 81, 1972.
- [14] D. Trbojevic *et al.*, "Design Method for High Energy Accelerator without Transition Energy", Proc. 2<sup>nd</sup> EPAC, Nice, p. 1536, 1990.
- [15] A. Sorensen, CERN Report MPS/Int. MU/EP 67-2 (1967) or Particle Accelerators **6**, 141 (1975).
- [16] W. Hardt and D. Möhl, "Q-jump at Transition", CERN ISR-300/GS/69-16, 1969.
- [17] D. Möhl, "Compensation of Space Charge Effects at Transition by an Asymmetric Q-jump – A

Theoretical Study”, CERN ISR-300/GS/69-62, 1969.

- [18] W. Hardt, Proc. 9<sup>th</sup> Int. Conf. on High Energy Accelerators (USAEC, Washington, DC, 1974).
- [19] E. Métral, “Stability Criteria for High-Intensity Single-Bunch Beams in Synchrotrons”, Proc. 8th EPAC, Paris, France, 3-7 June 2002.
- [20] T. Risselada, Proc. CERN Accelerator School, CERN-91-04, p. 161, 1991.
- [21] L.C. Teng, “Compensation of Space-Charge Mismatch at Transition of Booster using the Transition jump method”, FN-207, 17 April 1970.
- [22] M. Martini, “CERN PS  $\gamma_t$  Jump Scheme” The 1st mini-workshop on transition crossing (organized by the ICFA working group on High Intensity High Brightness Hadron Beams), May 20-23, 1996, Fermilab  
(<http://hadron.kek.jp/~icfa/workshops/workshops.html>).
- [23] M. Martini, CERN internal APC meeting, “PS transition crossing: transverse issues” 06/072006: <https://ab-div.web.cern.ch/ab-div/Meetings/APC/2006/apc060706/MM-APC06-07-2006.pdf>.
- [24] S. Hancock and E. Métral, “Ghost Bunches and Blow-Up Losses with High-Intensity Beams”, PS/RF Note 2002-198, November 2002.
- [25] E. Métral, CERN internal RLC meeting, “Crossing Transition with TMCI”, 19/09/2006: [http://ab-abp-rlc.web.cern.ch/ab-abp-rlc/Meetings/2006/2006.09.19/CrossingTransitionWithTMCI\\_RLC\\_19-09-06.pdf](http://ab-abp-rlc.web.cern.ch/ab-abp-rlc/Meetings/2006/2006.09.19/CrossingTransitionWithTMCI_RLC_19-09-06.pdf).